



Remarkable activity of Ag/Al₂O₃/cordierite catalysts in SCR of NO with ethanol and butanol



Pavlo Kyriienko^{a,*}, Nataliia Popovych^a, Sergiy Soloviev^a,
Svitlana Orlyk^a, Stanislaw Dzwigaj^{b,c}

^a L.V. Pisarzhevsky Institute of Physical Chemistry of the NAS of Ukraine, 31 Prosp. Nauky, 03028 Kyiv, Ukraine

^b UPMC Univ Paris 06, Laboratoire de Réactivité de Surface, Case 178, Site d'Ivry-Le Raphaël, 3 rue Galilée, 94200 Ivry sur Seine, France

^c CNRS-UMR 7197, Laboratoire de Réactivité de Surface, Case 178, Site d'Ivry-Le Raphaël, 3 rue Galilée, 94200 Ivry sur Seine, France

ARTICLE INFO

Article history:

Received 16 February 2013

Received in revised form 24 April 2013

Accepted 30 April 2013

Available online 9 May 2013

Keywords:

Silver–alumina

Cordierite

SCR of NO

Ethanol, Butanol

ABSTRACT

Structured silver–alumina catalysts were prepared by the one-step deposition of Al₂O₃ directly on the surface of cordierite block matrices with subsequent incipient wetness impregnation of Al₂O₃/cordierite with an AgNO₃ aqueous solution. The catalysts were characterized by BET, XRD, XPS and FTIR spectroscopy with CO and pyridine as molecule probe, diffuse reflectance UV–vis, TEM and SEM. The Ag/Al₂O₃/cordierite catalysts are highly active in SCR of NO with ethanol and butanol and very selective toward N₂. The conversion of NO over 0.6%Ag/45%Al₂O₃/cordierite catalyst reaches the high values of 95–99% already at 250 °C and remains at this high level up to 430 °C. The optimal silver loading in the silver–alumina catalysts is differing for C₂ and C₄ alcohols. It is shown that the role of silver in the Ag/Al₂O₃/cordierite catalyst consists in the modification of both redox and acid–base properties of the catalyst surface. Isolated cations (Ag⁺) and/or silver nanoclusters (Ag_n^{δ+}) contain adsorbed oxygen in quantities sufficient only for the partial oxidation of alcohols toward oxygenated compounds, which then reduce NO.

© 2013 Elsevier B.V. All rights reserved.

1. Introduction

Selective catalytic reduction (SCR) of NO_x with hydrocarbons and oxygenates has remained among intense research processes of environmental catalysis as a promising method for abatement of nitrogen oxides in the gas emissions of diesel and lean-burning engines [1–7]. Among the various catalytic systems proposed for SCR of NO with organic reducing agents silver–alumina catalysts stand out for the high activity, selectivity to N₂ [1,8–12] and resistance to SO_x [13,14]. Oxygenates are considered as prospective organic reducing agents of NO_x because they are more active than hydrocarbons [8,15–18] and can be used as components of engine fuel (e.g. ethanol, butanol) [19–21].

Structured catalysts with active catalytic compositions supported on ceramic or metallic block matrices are generally used in the processes of gas purification [22,23]. The formation of a layer of active phase with required physicochemical properties on a block matrix is one of the most difficult problems in these catalysts developing. The activity of structured Ag/Al₂O₃ catalysts in the process of SCR of NO_x with ethanol, described in several reports [2,24–26], is lower than bulk catalysts. Therefore, it is required to develop a

method for coating of ceramic block matrices with alumina, which are characterized by own SCR activity, in order to obtain highly active structured Ag/Al₂O₃ catalysts.

The disadvantages of existing preparation technique of structured silver–alumina catalysts by multiple dipping of block matrices into washcoat slurries (Ag/Al₂O₃) are as follows: change in macroporosity, blocking of bottom layers of active phase, a complementary binding agent and additional power inputs. Also expensive precursors are required for deposition of Al₂O₃ from solution of aluminum salts by the sol–gel technique.

In this work one-step method is developed for coating of block cordierite matrices with a mesoporous alumina. The activity of the Ag/Al₂O₃/cordierite catalysts is investigated in the process of SCR of NO_x with ethanol and butanol. A special focus is directed on the influence of silver on the acid–base properties of the Ag/Al₂O₃ catalysts and the effect of silver loading on the catalytic properties.

2. Experimental

2.1. Catalysts preparation

Ceramic block matrices with a honeycomb structure of synthetic cordierite (2Al₂O₃·2MgO·5SiO₂) were used as catalyst supports. The catalyst surface was formed by coating with Al₂O₃ from aqueous solution of KOH with aluminum swarf. Formed in the

* Corresponding author. Tel.: +380 44 5256222; fax: +380 44 5256590.

E-mail address: pavlo.kyriienko@ukr.net (P. Kyriienko).

process of dissolution $K(Al(OH)_4)$ was easily hydrolyzed (with polycondensation and polymerization) and aluminum hydroxide was deposited on the surface of cordierite matrix (labeled as CM). After that, samples were dried in air at 110°C with subsequent calcination in air at 600°C . The catalysts were prepared by incipient wetness impregnation of Al_2O_3/CM with an $AgNO_3$ aqueous solution. Then samples were dried in air at 110°C and calcined at 600°C . Several samples of $Ag/Al_2O_3/CM$ were prepared with silver loading of 0.3, 0.6, 1.0 and 1.5 wt.% and alumina loading of 45 wt.%.

2.2. Catalysts characterization

The textural properties were studied on Sorptomatic 1990 apparatus at -196°C using nitrogen adsorption/desorption method. The samples were degassed under vacuum for 3 h at 130°C prior to measurements. The specific surface area of samples was determined by the Brunauer–Emmett–Teller (BET) method. The mesopore size distribution was obtained by the Barrett–Joyner–Halenda (BJH) method.

X-ray diffraction (XRD) patterns of the powder samples were recorded using D8 Advance (Bruker AXS GmbH, Germany) diffractometer with monochromatized $Cu-K_\alpha$ radiation (nickel filter, $\lambda = 0.15184\text{ nm}$).

The morphology of the sample surface was studied using transmission electron microscope (TEM) Selmi TEM-125K (Selmi, Ukraine) and scanning electron microscope (SEM) JSM 6700F (JEOL, Japan).

Analysis of the acid properties of samples was performed by adsorption of CO and pyridine followed by infrared spectroscopy. Before analysis, the samples were pressed at $\sim 1\text{ ton cm}^{-2}$ into thin wafers of ca. 10 mg cm^{-2} and placed inside the IR cell.

Fourier Transform Infrared (FTIR) spectra with pyridine were recorded on Spectrum One FTIR spectrometer (Perkin Elmer, USA) accumulating 12 scans at a spectral resolution of 1 cm^{-1} . The cell was connected to a vacuum-adsorption apparatus allowing a residual pressure below 10^{-3} Pa . The spectra were recorded under ambient conditions after pyridine desorption at 50, 100, 150, 250 and 350°C . Before pyridine adsorption, the samples were outgassed (10^{-3} Pa) at 400°C for 1 h.

Before CO adsorption experiment, the wafers were activated by calcination at 450°C for 2 h in flowing 2.5% O_2/Ar and then outgassed at 300°C (10^{-3} Pa) for 1 h. Following thermal treatment, the samples were cooled down to -173°C . CO was introduced in increasing amounts up to an equilibrium pressure of 133 Pa. Infrared spectra were recorded using Bruker Vertex 70 spectrometer (resolution 2 cm^{-1} , 128 scans). The spectra were obtained after subtraction of the spectrum recorded after calcination and prior to CO adsorption. When necessary, the contribution of CO in the gas phase was removed by subtraction of the gas-phase spectrum.

UV–vis diffuse reflectance spectra were recorded under ambient conditions on Specord M40 (Carl Zeiss, Germany) with a standard diffuse reflectance unit.

X-ray photoelectron spectroscopy (XPS) measurements were performed with a hemispherical analyzer (PHOIBOS 100, SPECS GmbH) using $Mg-K_\alpha$ (1253.6 eV) radiation. The power of the X-ray source was 300 W. The grinded block fragment was pressed on an indium foil and mounted on a special holder. Before the analysis, $Ag/Al_2O_3/CM$ sample were outgassed at room temperature to a pressure of 10^{-7} Pa . All spectra were fitted with a Voigt function (a 70/30 composition of Gaussian and Lorentzian functions) in order to determine the number of components under each XPS peak.

2.3. Catalytic activity measurement

Catalytic activity tests were carried out in a fixed-bed flow quartz reactor at atmospheric pressure. Catalyst block

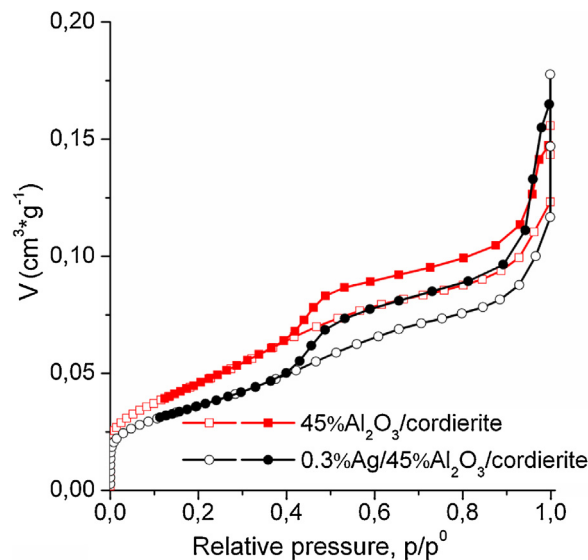


Fig. 1. Adsorption isotherms of nitrogen on catalysts at -196°C . Empty symbols – adsorption; full symbols – desorption. For convenience, the dataset for $45\%Al_2O_3/CM$ sample was shifted upwards along the Y-axis.

fragment (8 mm in diameter $\times 8\text{ mm}$ in length (0.4 cm^3) with density 49 cells cm^{-2} , 0.45 g) was placed in the reactor. The composition of the reaction mixture (gas feed): 500 ppm NO, 1000 ppm C_2H_5OH (or 500 ppm $n-C_4H_9OH$), 10% O_2 (6% H_2O) in He, at the flow rate of $200\text{ cm}^3\text{ min}^{-1}$ (GHSV is $30,000\text{ h}^{-1}$). The gas feed was adjusted by mass-flow controllers (Chromatek-Crystal FGP). Water vapor was introduced into the reaction system by passing He through a saturator with deionized water. Before the reaction, the catalyst was heated up to 600°C with a heating rate of $20^\circ\text{C min}^{-1}$ in a flow of reaction mixture and held for 1 h, then was cooled to 180°C with a further step-heating to a temperature of conversion measurement. The steady-state activity was measured in the temperature range of $200\text{--}500^\circ\text{C}$ after 30 min reaction at a certain temperature. The temperature was controlled through an Autotronics TZN4S temperature controller using a Chromel–Alumel thermocouple. The concentration of NO was continuously monitored using a chemiluminescence gas analyzer (344HL04, Ukraine). The products were analyzed by gas chromatograph (TCD) (Kristal-lyuks 4000M, Metachrom, Russia) with a CaA column (for NO, N_2 , CO) and a Polisorb-1 column (for N_2O , CO_2 , ethanol, butanol). Catalytic activity was characterized by NO conversion and temperatures of its achievement. Conversion of NO was calculated as $X(NO) = (1 - [NO]_{out}/[NO]_{in}) \cdot 100$, where the subscript “in” refers to initial concentration whereas “out” means after reaction.

3. Results and discussion

3.1. Structural and textural characteristics of the catalysts

Adsorption and desorption isotherms of nitrogen show that the cordierite-supported alumina is a mesoporous material (Fig. 1). The presence of mesopores is confirmed by data obtained by small-angle XRD analysis (Fig. 2A). Micropores in this material are almost absent. Specific surface area is $45\text{ m}^2/\text{g}$. Average size of mesopores is 3 nm. There are insignificant differences ($\pm 3\%$) in the surface area and the size of pores after silver doping.

According to XRD patterns (Fig. 2B) the alumina is a mixture of $\gamma-Al_2O_3$ and $\eta-Al_2O_3$ phases ($2\theta = 19.4^\circ$ (1 1 1); 37.2° (3 1 1); 45.6° (4 0 0); 66.9° (4 4 0)). However, it is difficult to discriminate these phases by XRD because similarity in their structures leads to a coincidence of diffraction peaks [27]. The difference is observed in the

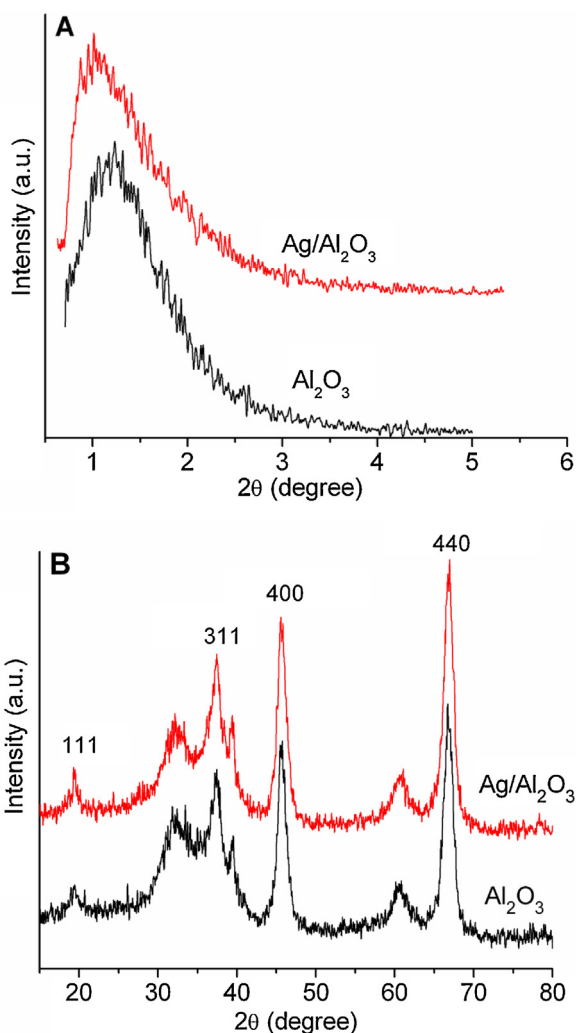


Fig. 2. XRD of Al₂O₃ and 2%Ag/Al₂O₃.

shape and intensity of (1 1 1) peak: narrow for η -Al₂O₃ and less pronounced broad peak for γ -Al₂O₃ [27,28]. The form of (1 1 1) diffraction peak (Fig. 2B) is a superposition of two components; broad base and narrow peak also indicate the lamellar particles of alumina [27]. Coherent-scattering region of the alumina is 13 nm calculated by Scherrer equation for (4 4 0) peak. Structural changes of alumina have not been revealed after silver doping according to XRD (Fig. 2B). A silver phase is not detected due to the low silver loading in consistent with [6].

Fig. 3 shows the TEM of alumina (A) and silver–alumina with different Ag loading (B – 0.6 wt.% of Ag approximately corresponds to the active phase of 0.3%Ag/45%Al₂O₃/CM, C – 2.0 wt.% of Ag as the active phase of 1.0%Ag/45%Al₂O₃/CM). These micrographs exhibit that the samples are porous nanosized materials. For 0.6%Ag/Al₂O₃ no clear silver particles are visible, so one can conclude that silver is uniformly distributed over the surface of Al₂O₃. It can be clearly seen that increase of the silver loading up to 2.0 wt.% of Ag leads to the formation of silver particles of 10–30 nm on the alumina surface (Fig. 3C). The insets in Fig. 3B and C are the electron diffraction patterns of the silver–alumina samples. The values of interplaner spacings (d_{hkl}) calculated from the diameters of the electron diffraction rings are compared with the standard ASTM data. In both samples the most contrast electron diffraction spots/rings can be attributed to the (1 1 1), (2 0 0), (2 2 0) planes of the face-centered cubic metallic silver (Ag) and (1 1 1) plane of silver oxide (Ag₂O).

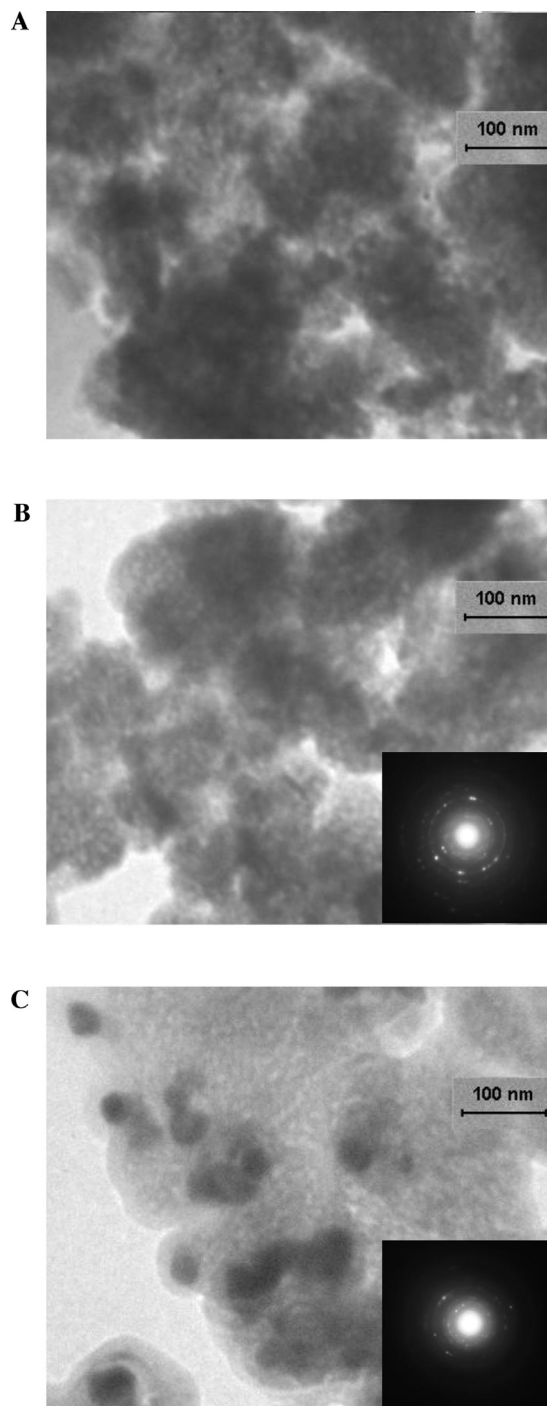


Fig. 3. TEM images of Al₂O₃ (A), 0.6%Ag/Al₂O₃ (B) and 2%Ag/Al₂O₃ (C).

According to SEM image of 1.0%Ag/45%Al₂O₃/CM sample, thickness of the cordierite-supported alumina layer is about 90 μ m (Fig. 4A). The catalytic coating is uniformly distributed over the surface of cordierite and consists of the lamellar particles (Fig. 4B).

3.2. Acid–base characteristics of the catalysts surface

The surface hydroxyls of 0.3%Ag/45%Al₂O₃/CM catalyst were identified at the IR spectrum in the OH stretching region of 3900–3000 cm^{-1} (Fig. 5A). The peak at 3756 cm^{-1} is assigned to terminal OH-groups which associated with octa-coordinated aluminum atoms – Al_{OH}OH (where Al_{OH} states for an octa-coordinated

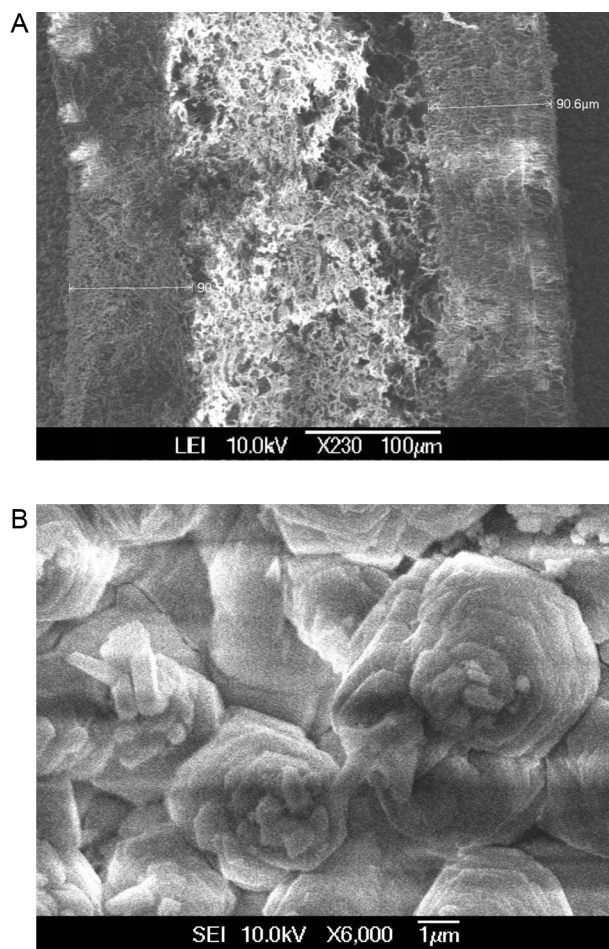


Fig. 4. SEM images of 1.0%Ag/45%Al₂O₃/CM.

aluminum atom). The peaks at 3730 and 3680 cm⁻¹ are assigned to bridging OH-groups between two aluminum atoms Al_{OH}OHAL_{OH} (3730 cm⁻¹) and Al_{OH}OHAL_{Th} (3680 cm⁻¹) (where Al_{Th} states for a tetra-coordinated aluminum atom) and the peak at 3587 cm⁻¹ is assigned to hydrogen bonded OH groups [29,30].

When hydroxyls interact with CO by H-bonding, a shift of the corresponding O–H stretching band occurs, with formation of a new IR absorption band at lower wavenumbers. The higher the OH acidity, the larger is the shift of the OH modes [29]. In the present case, introduction of CO (100 Pa equilibrium pressure) at –173 °C leads to an erosion of the original hydroxyl bands and appearance of the intense bands at 3656, 3625 and 3565 cm⁻¹ (Fig. 5A). Their intensities quickly decrease with the CO equilibrium pressure, while the bands at 3756, 3730 and 3680 cm⁻¹ are restored. The observed shifts of 100 cm⁻¹ for terminal OH-groups, 105 and 115 cm⁻¹ for bridging OH-groups indicate a weak acidity of the surface hydroxyls on 0.3%Ag/45%Al₂O₃/CM sample.

Fig. 5B shows the changes in the carbonyl region when CO is adsorbed on 0.3%Ag/45%Al₂O₃/CM. For convenience, the same set of spectra as that presented in Fig. 5A is given. Under CO equilibrium pressure of 100 Pa, carbonyl bands are detected at 2153, 2158, 2165, 2170, 2185 and 2193 cm⁻¹ (Fig. 5B, spectrum a). The bands at 2165, 2158 and 2153 cm⁻¹ change simultaneously with a red shift of the bands at 3756, 3730 and 3680 cm⁻¹ (see Fig. 5 A and B) and are, therefore, assigned to CO attached to terminal and bridging OH-groups.

Further outgassing provokes disappearance of the carbonyl band at 2185 cm⁻¹ with a shift to 2188 cm⁻¹. Two bands at 2198 and 2170 cm⁻¹ are well resolved at relatively low CO coverages. These

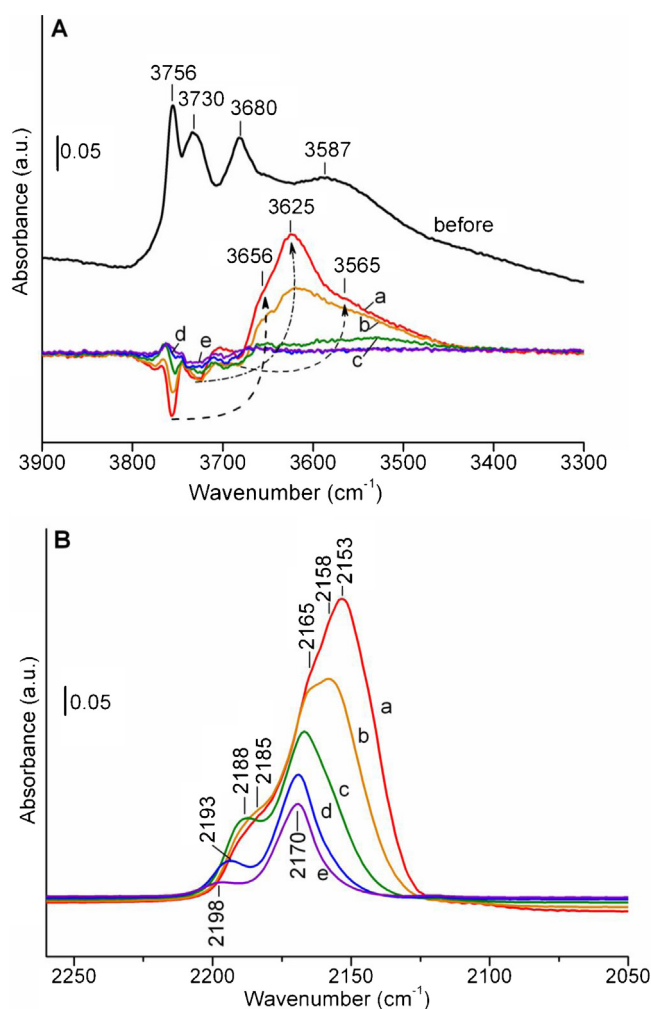
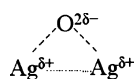


Fig. 5. FTIR spectra ((A) OH stretching region and (B) carbonyl stretching region) of 0.3%Ag/45%Al₂O₃/CM after adsorption of CO at –173 °C: equilibrium CO pressure of 100 Pa (a) and development of the spectra during evacuation (10 Pa (b), 10⁻² Pa (c), 10⁻³ Pa (d), 10⁻⁴ Pa (e)).

bands, as well as the band at 2185 cm⁻¹, do not correlate with any OH bands and are thus assigned to aluminum and silver carbonyls. Therefore, two types of Lewis acid sites (LAS) have been identified on the surface of the silver–alumina sample: octa-coordinated aluminum atoms with one vacant coordinate site and others occupied by oxygen atoms (peaks at 2198–2185 cm⁻¹) and LAS formed by silver ions (peak at 2170 cm⁻¹) [29].

Results of investigation of Al₂O₃ and Ag/Al₂O₃ surfaces by FTIR-spectroscopy with pyridine have shown that spectrum of 0.6%Ag/Al₂O₃ is characterized by the similar intensity of peaks at 1450 and 1616 cm⁻¹ and new peaks detected at 1456 and 1625 cm⁻¹ which are almost absent on Al₂O₃ (Fig. 6). It should also be noted that these new peaks have remained under desorption temperature of 350 °C. So, amount and strength of LAS have increased after doping of alumina with silver. These results are accorded with the foregoing data of FTIR spectroscopy with CO. According to [31], formation of silver LAS on Ag/Al₂O₃ surface may occur due to the interaction of silver with the gas phase oxygen or oxygen of alumina lattice. Adsorbed oxygen in this case is a conjugated base, i.e. Lewis conjugated acid–base pairs are formed on the oxidized silver surface:



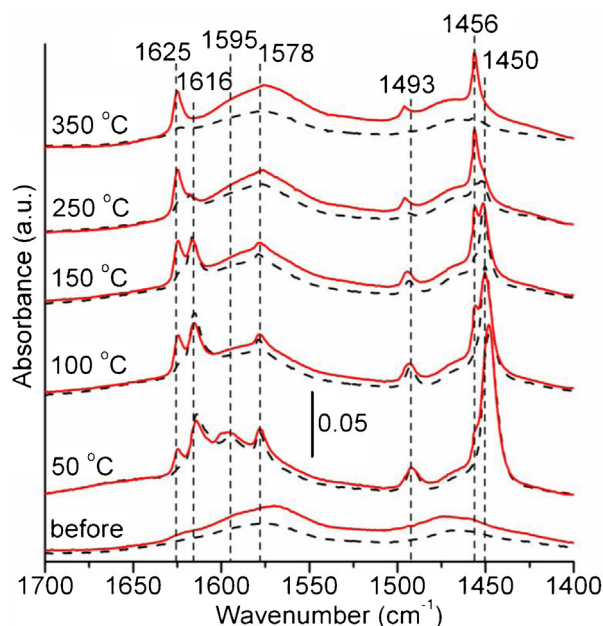


Fig. 6. FTIR spectra recorded at room temperature of pyridine adsorbed at 50 °C and then desorbed at 50, 100, 150, 250 and 350 °C on the sample of Al_2O_3 (dashed line) and 0.6%Ag/ Al_2O_3 (straight line).

It is known that LAS act as adsorption centers for alcohols that are very important in reductant activation on the catalyst surface (the role of LAS in NO SCR with alcohols will be discussed in more detail in Section 3.5).

3.3. Structure and valence state of silver in the catalysts

The UV–vis spectra of 0.3%Ag/45% Al_2O_3 /CM and 1.0%Ag/45% Al_2O_3 /CM samples before and after the SCR-reaction are shown in Fig. 7. Absorption bands (a.b.) at 210, 240–288, 340 and 423 nm are observed. The a.b. at 210 nm is generally attributed to highly dispersed Ag^+ cations (electronic transitions $\text{Ag}^+([\text{Kr}]4d^{10}) + h\nu \rightarrow \text{Ag}^+([\text{Kr}]4d^9 5s^1)$), the a.b. in the range of 240–288 nm are commonly ascribed to silver nanoclusters $\text{Ag}_n^{\delta+}$ ($n \leq 8$) with a variety of cluster sizes and/or different oxidation states, the a.b. at 340 and 423 nm are assigned to larger silver nanoclusters ($n > 8$) and metallic silver nanoparticles, respectively [32–35].

It should be emphasized that decreasing of a.b. intensity at 210–252 nm in the UV–vis spectrum of 1.0%Ag/ Al_2O_3 /CM catalyst has been observed after the SCR reaction with increasing of a.b. intensity at 423 nm. It suggests that sintering of silver particles has taken place in the reaction conditions. In contrast, for 0.3%Ag/ Al_2O_3 /CM catalyst intensity of a.b. before and after reaction is not changed. Therefore increase of silver loading in Ag/ Al_2O_3 /cordierite catalyst results in the sintering of silver nanoparticles which are known to catalyze the deep oxidation of reductant, in line with earlier works [36,37].

Considering the obtained DR UV–vis results one can suggest that silver nanoparticles in Ag/ Al_2O_3 /CM catalysts upon SCR of NO reaction may agglomerate due to the reduction of oxidized silver, melt (silver clusters are characterized by lower melting temperature than metallic silver [38]) and diffuse over alumina surface under the reaction conditions. If silver clusters are close enough to each other, they could sinter and agglomerate. The silver nanoclusters in 0.3%Ag/ Al_2O_3 /CM catalyst are more dispersed than those in 1.0%Ag/ Al_2O_3 /CM, therefore in UV–vis spectrum of 0.3%Ag/ Al_2O_3 /CM intensity of a.b. at 210–252 nm has not decreased after SCR-reaction. The increasing of the silver species size in the

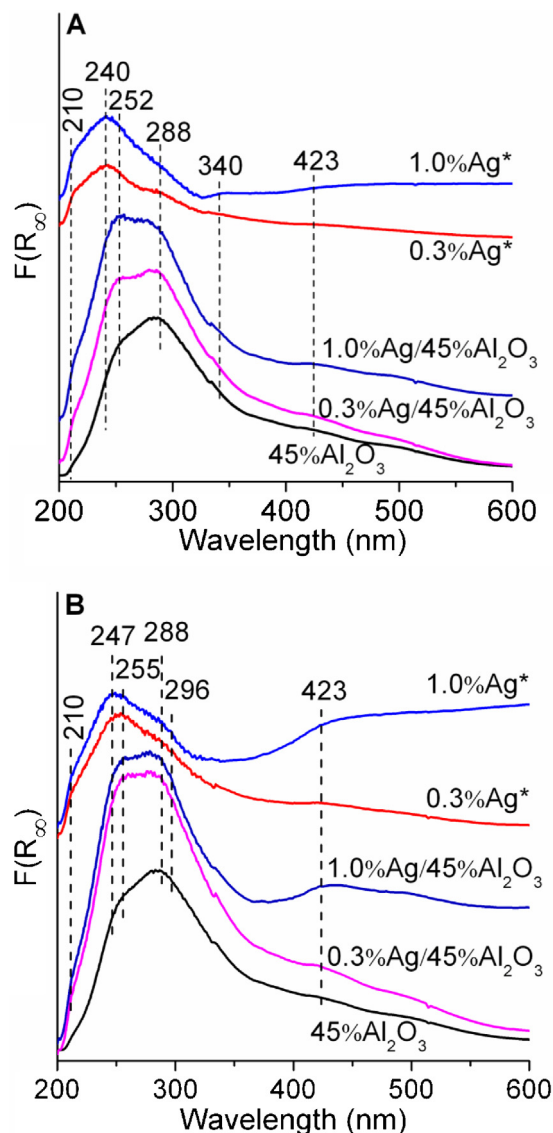


Fig. 7. DR UV–vis spectra of cordierite-supported samples before (A) and after (B) SCR-reaction recorded at ambient atmosphere (* spectra – obtained by subtraction of Ag/45% Al_2O_3 /CM from 45% Al_2O_3 /CM).

catalysts with higher silver loading is in agreement with the above stated TEM results.

The presence of different valence states of silver in the Ag/ Al_2O_3 /CM samples (after SCR-reaction) has been confirmed by the XPS (Fig. 8). Deconvolution of the $\text{Ag}3d_{5/2}$ peaks shows the presence of two contributions at 368.6–368.7 and 367.9 eV attributed, according with literature [39], to Ag^0 and Ag^+ (as for Ag_2O), respectively. As seen, the position of $\text{Ag}3d_{5/2}$ bands is practically unchanged with the increase of silver loading in the catalyst from 0.6 to 1.5 Ag wt.% while intensity of the bands is increased.

3.4. Catalytic properties

Fig. 9 shows the temperature dependences of NO conversions in the SCR of NO with ethanol and butanol over the Ag/ Al_2O_3 /CM with different silver loadings. It can be seen that prepared catalysts are highly active in the SCR reaction as shown by 95–99% conversions of NO achieved already at 250–270 °C over the most active catalysts. It should be noted that the SCR activity of Ag/ Al_2O_3 /cordierite

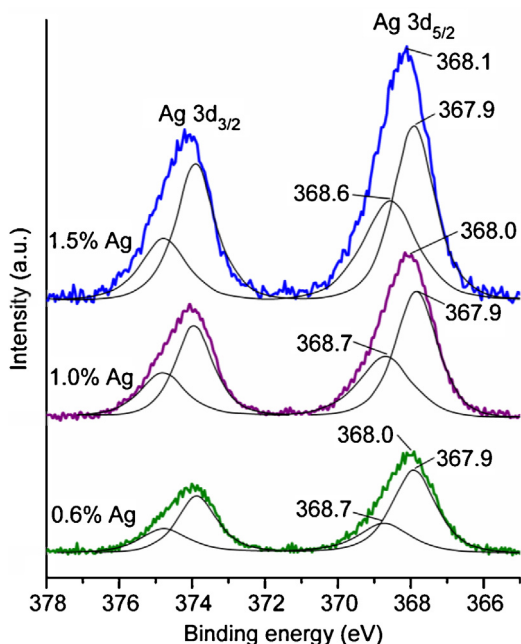


Fig. 8. XPS spectra recorded at room temperature of spent Ag/45%Al₂O₃/CM catalysts with different silver loading (0.6, 1.0, 1.5 wt.%) after SCR of NO with ethanol, outgassed (10⁻⁷ Pa) at room temperature.

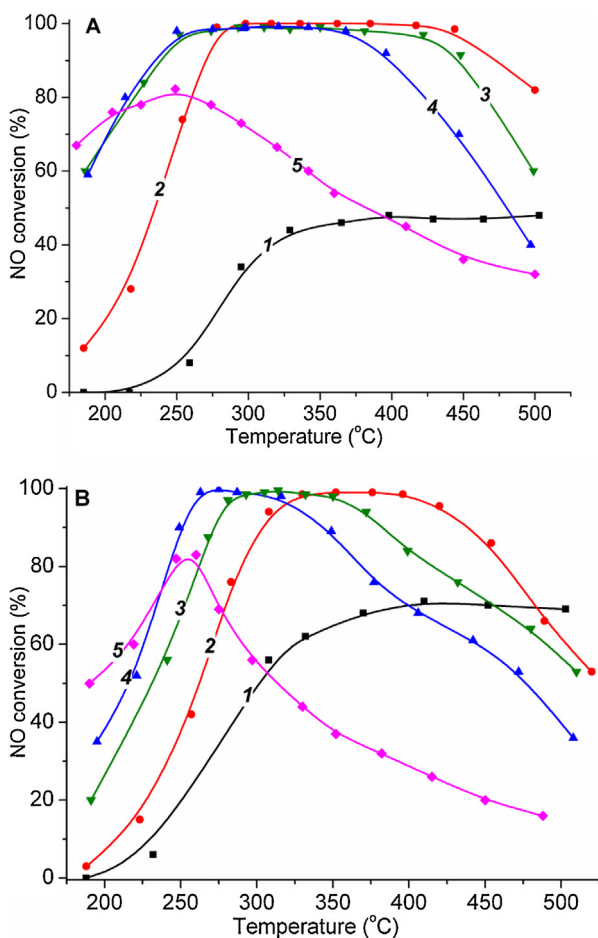


Fig. 9. Dependence of NO conversion on temperature in SCR of NO with ethanol (A) and butanol (B) over 45%Al₂O₃/CM (1) and Ag/45%Al₂O₃/CM catalysts with silver loading (wt.%): 0.3 (2), 0.6 (3), 1.0 (4), and 1.5 (5).

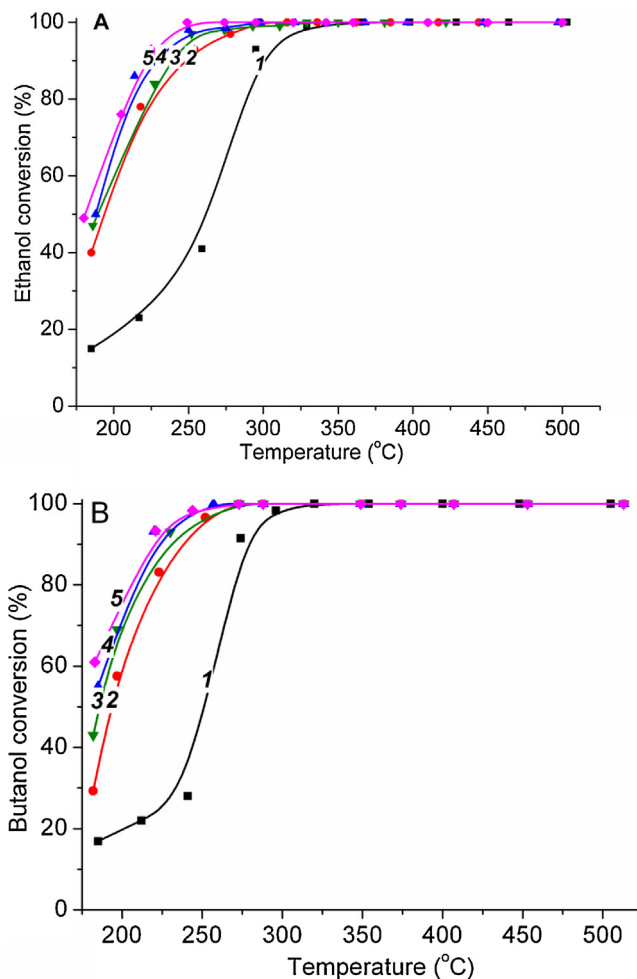


Fig. 10. Dependence of ethanol (A) and butanol (B) conversion on temperature in SCR of NO with ethanol and butanol over 45%Al₂O₃/CM (1) and Ag/45%Al₂O₃/CM catalysts with silver loading (wt.%): 0.3 (2), 0.6 (3), 1.0 (4), and 1.5 (5).

catalysts in close conditions described in [2,24–26] was lower: 87–90% NO conversion at 380–400 °C. So we can conclude that new preparation method of structured Ag/Al₂O₃/CM catalysts for the SCR of NO_x with alcohols is highly effective.

High conversions of ethanol and butanol over Ag/Al₂O₃/CM catalysts in the SCR process insignificantly depend on the silver loading. The temperatures of complete conversion of ethanol and butanol are similar and equal to 250–270 °C (Fig. 10).

In NO SCR process by ethanol, the most active catalyst is 0.6%Ag/Al₂O₃/CM on which 95–99% conversion of NO is achieved at 250 °C (Fig. 9A, curve 3) and remains on the same level up to 430 °C, i.e. in the temperature range (Δt) of 180 °C. Over 0.3%Ag/Al₂O₃/CM and 1.0%Ag/Al₂O₃/CM catalysts, conversion of NO in the SCR reaction is 95–99% in the temperature range of 275–455 °C (Fig. 9A, curve 2) and 245–380 °C (Fig. 9A, curve 4), respectively. The conversion of NO is only 80% at 250 °C in the SCR reaction over 1.5%Ag/Al₂O₃/CM. The observed order of the catalysts activity in the selective reduction of NO with ethanol based on the temperature range of the high NO conversion is: 0.3%Ag ($\Delta t = 180$ °C) \approx 0.6%Ag ($\Delta t = 180$ °C) $>$ 1.0%Ag ($\Delta t = 135$ °C).

Activities of Ag/Al₂O₃/CM catalysts with different silver loading in the process of SCR of NO with butanol (Fig. 9B) differ more significantly (by the temperature range of maximum NO conversions) than in the case of SCR of NO with ethanol (Fig. 9A). The most active catalyst is 1.0%Ag/Al₂O₃/CM on which 95–99% conversion

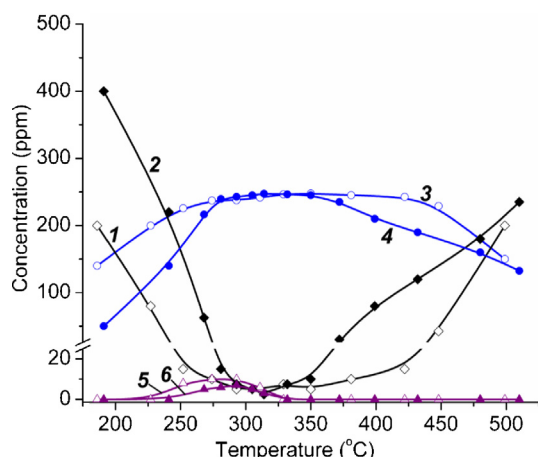


Fig. 11. Temperature dependences of concentration changing of NO (1 and 2), N_2 (3 and 4) and N_2O (5 and 6) in SCR of NO with ethanol (1, 3 and 5) and butanol (2, 4 and 6) over 0.6%Ag/45%Al₂O₃/CM catalyst.

of NO is achieved at 255 °C (Fig. 9B, curve 4). The NO conversions of 95–99% are achieved also over the catalysts with lower silver loading (0.3 and 0.6 Ag wt.%) but at higher temperatures. In the case of 1.5%Ag/Al₂O₃/CM catalyst, maximum conversion of NO is achieved at 250 °C, but it is only 80% as well as in the case of SCR with ethanol. The observed order of the catalysts activity in the selective reduction of NO with butanol based on the temperature range of the high NO conversion is: 0.3%Ag (315–420 °C, $\Delta t = 105$ °C) > 0.6%Ag (280–365 °C, $\Delta t = 85$ °C) > 1.0%Ag (255–325 °C, $\Delta t = 70$ °C).

Fig. 11 shows the temperature dependences of concentration changing of NO, N_2 and N_2O in the SCR of NO with ethanol and butanol over 0.6%Ag/Al₂O₃/CM. As can be seen, prepared catalysts are highly selective to N_2 in the SCR-process.

The addition of water vapor into the reaction mixture leads to an insignificant decrease of maximum NO conversion over 0.6%Ag/Al₂O₃/CM in the SCR-process with ethanol and butanol (Fig. 12). This may be due to the fact that water (as well as alcohol) is Lewis base and can be adsorbed on Lewis acid sites (silver) after reductant activation. It is worth noting that the effect of H₂O is reversible: when the addition of water vapor to the reaction mixture was stopped, the NO conversion recovered to its initial level. The effect of water vapor on the activity of these catalysts will be a subject of our further studies.

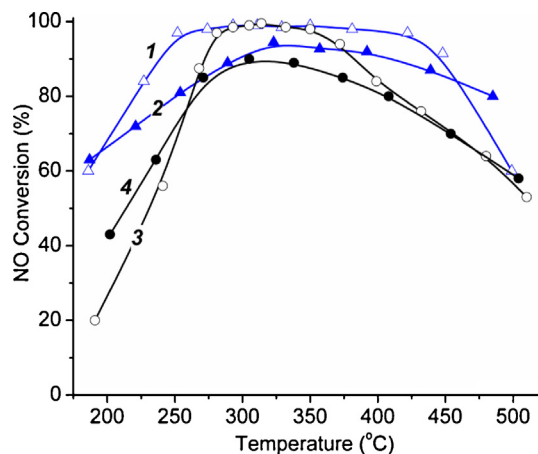
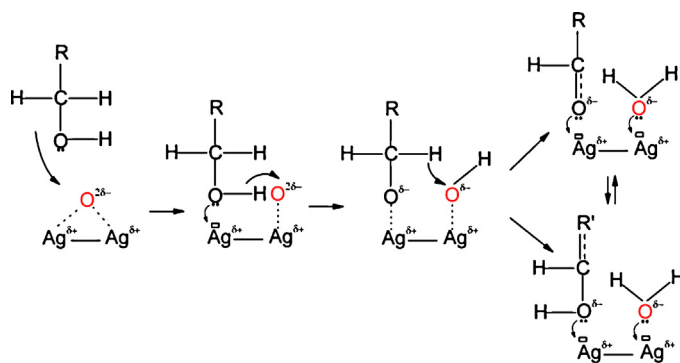


Fig. 12. Temperature dependences of NO conversion in SCR with ethanol (1 and 2) and butanol (3 and 4) over 0.6%Ag/45%Al₂O₃/CM (without H₂O (1 and 3) and with H₂O (2 and 4)).



Scheme 1. Representation of possible alcohols activation (adsorption and partial oxidation to enolic or aldehyde species) on silver (Lewis acid sites).

3.5. Active sites of Ag/Al₂O₃ catalysts for SCR of NO with C₂ and C₄-alcohols

Let us consider in more detail the role of silver active sites of Ag/Al₂O₃ catalysts in the SCR of NO with C₂ and C₄ alcohols. It is known that NO_x activation occurs on the surface of alumina with the formation of adsorbed monodentate, bidentate and bridging nitrate species [9,40]. Since NO is reduced with ethanol and butanol even on the silver-free alumina (Fig. 9, curves 1), we can conclude that the activation of alcohols can occur on LAS of alumina due to the alcohols dehydrogenation [41]. The impregnation of silver precursor on alumina leads to increase of the amount and strength of LAS (as confirmed by FTIR-spectroscopy with CO and pyridine) and as a result strongly increases the activity of alumina catalyst. Thus, it seems that role of silver (Ag⁺ cations and Ag_n^{δ+} nanoclusters) consists in the activation of alcohols, adsorbed on LAS which include silver, by their partial oxidation with formation of more reactive intermediates (enolic species) [2,42–44]. The effect of silver on Brønsted acidity and total acidity (NH₃-TPD) of Ag/Al₂O₃ and their influence on the catalytic activity were also pointed in earlier works [45,46]. On the other hand, it is known that the partial oxidation of primary alcohols occurs on the relatively large particles of metallic silver coated with the oxide film (e.g. industrial catalysts for the oxidation of methanol to formaldehyde, ethylene glycol to glyoxal) [32]. Thus, silver species in Ag/Al₂O₃/cordierite form both redox and acid–base catalytic active sites and provide bifunctional character of the catalyst. Taking into account data obtained in this work and earlier studies of the mechanism of alcohols activation on silver [31,42–44,47,48], we proposed a possible way (Scheme 1) of activation of alcohols (as Lewis bases) on silver Lewis acid sites of catalyst with the formation of enolic or aldehyde species.

The effect of silver loading on the catalysts activity in the process of NO SCR may be related to the amount of chemisorbed oxygen on different silver species. It is known that selective reduction of NO is dependent on the partial oxidation of the organic reductant, which in turn is dependent on the C–H (or C–C) bond strength, accessibility of p-electrons, molecular orientation and sticking probability of the hydrocarbon reductant [49]. Also level of reductant oxidation (partial, deep) is dependent on the amount and bond strength of chemisorbed oxygen with the catalyst surface [50]. It seems that isolated Ag⁺ cations and Ag_n^{δ+} nanoclusters adsorb oxygen in quantities sufficient only for the partial oxidation of alcohols. Further adsorption of oxygen on these sites is sterically impossible while products of partial oxidation are on them. The release of silver sites is possible either after interaction of these products with NO_x adsorbed on adjacent sites of alumina (i.e. SCR-reaction [9,40,51]) or after desorption of products of partial oxidation. Amount of adsorbed oxygen on larger particles of metallic silver is greater and it is favored to the deep oxidation of the alcohols to CO_x and

H₂O [8,36]. Besides, on these silver particles interaction of activated reductant with chemisorbed oxygen is more probable than with NO_x species adsorbed on alumina. In our experiments, when silver loading is risen from 0.3 to 1.0%, content of larger silver nanoclusters is increased (according to the UV–vis spectroscopy, Fig. 7) with the simultaneous increasing of the amount of chemisorbed oxygen. A further increase of silver loading leads to the formation of larger particles of metallic silver with higher amount of chemisorbed oxygen, which promotes the deep oxidation of reducing agent to CO_x and H₂O [8,36,37,51]. This is in line with the lower activity of the 1.5%Ag/Al₂O₃/CM catalyst (Fig. 9) in the SCR of NO with ethanol and butanol.

The possible reasons of different dependence of activity of Ag/Al₂O₃/cordierite catalysts on silver loading in the SCR of NO with ethanol and butanol can be examined under views on the process mechanism. According to [6,14,42], in SCR of NO_x with ethanol organo-nitrogen intermediate complexes (R-ONO, R-NO₂, where R: ·C₂H₅), formed during the reaction of enolic and nitrate species, are transformed into the key intermediate –NCO species. During the decomposition of organo-nitrogen compounds formed of butanol molecule (R-ONO, R-NO₂, where R: ·C₄H₉), –NCO species can be formed together with hydrocarbon fragments which have C–C bonds (the importance of C–C bonds for reductant of NO in the SCR-reaction was shown in [49,52]). Then these hydrocarbon fragments either may be oxidized to CO₂ and H₂O or form oxygenates which are reactive in the SCR of NO_x. Thus, the greater the number of carbon atoms in the alcohol molecule, the higher the amount of oxygen chemisorbed on the surface of silver nanoclusters is required for the formation of oxygenates.

4. Conclusions

Structured silver–alumina catalysts prepared by the one-step deposition of Al₂O₃ directly on the surface of cordierite block matrices with subsequent incipient wetness impregnation of Al₂O₃/cordierite with an AgNO₃ aqueous solution are characterized by remarkable catalytic properties in the SCR of NO with ethanol and butanol.

The physicochemical properties of x%Ag/45%Al₂O₃/cordierite catalysts (with x = 0.3, 0.6, 1.0 and 1.5 Ag wt.%) were characterized by BET, XRD, XPS, FTIR spectroscopy with CO and pyridine as molecule probe, diffuse reflectance UV–vis, TEM and SEM.

Ag/Al₂O₃/cordierite catalysts are highly active in SCR of NO with ethanol and butanol and very selective toward N₂. The conversion of NO over 0.6%Ag/45%Al₂O₃/cordierite catalyst reaches the high values of 95–99% at 250 °C and remains at this high level up to 430 °C.

The optimal silver loading in Ag/Al₂O₃/cordierite catalysts depends on the kind of alcohol used as reducing agent.

The role of silver in Ag/Al₂O₃/cordierite catalyst consists in the modification of both redox and acid–base properties of the catalyst surface.

It seems that isolated cations (Ag⁺) and/or silver nanoclusters (Ag_n^{δ+}) contain adsorbed oxygen in quantities sufficient only for the partial oxidation of alcohols toward oxygenated compounds, which then reduce NO.

Acknowledgments

This work was financially supported by programs of National Academy of Sciences of Ukraine “Fundamental problems of nanostructure systems, nanomaterials, nanotechnologies” and “Fundamental problems of development of new substances and materials for chemical industry”, grant of National Academy of Sciences of Ukraine for implementation of research projects of young

scientists. Special thanks are due to C. Méthivier and J.M. Krafft (Laboratoire de Reactivité de Surface, Paris) for performing, respectively, the XPS and FTIR measurements (with CO) and P.S. Yaremov (L.V. Pisarzhevsky Institute of Physical Chemistry of the NASU, Kyiv) for performing nitrogen adsorption/desorption measurement.

References

- [1] J.P. Breen, R. Burch, C. Hardacre, C.J. Hill, B. Krutzsch, B. Bandl-Konrad, E. Jobson, L. Cider, P.G. Blakeman, L.J. Peace, M.V. Twigg, M. Preis, M. Gottschling, *Applied Catalysis B* 70 (2007) 36–44.
- [2] H. He, Y. Li, X. Zhang, Y. Yu, C. Zhang, *Applied Catalysis A* 375 (2010) 258–264.
- [3] K.I. Shimizu, M. Tsuzuki, A. Satsuma, *Applied Catalysis B* 71 (2007) 80–84.
- [4] K. Shimizu, K. Sawabe, A. Satsuma, *Catalysis Science & Technology* 1 (2011) 331–341.
- [5] S.N. Orlik, T.V. Mironyuk, T.M. Boichuk, *Theoretical and Experimental Chemistry* 48 (2012) 73–97.
- [6] H. He, Y. Yu, *Catalysis Today* 100 (2005) 37–47.
- [7] S.N. Orlik, *Catalysis Today* 191 (2012) 79–86.
- [8] T. Miyadera, *Applied Catalysis B* 2 (1993) 199–205.
- [9] S. Kameoka, Y. Ukisu, T. Miyadera, *Physical Chemistry Chemical Physics* 2 (2000) 367–372.
- [10] F. Klingstedt, K. Eränen, L.-E. Lindfors, S. Andersson, L. Cider, C. Landberg, E. Jobson, L. Eriksson, T. Ilkenhans, D. Webster, *Topics in Catalysis* 30/31 (2004) 27–30.
- [11] Y.H. Yeom, M. Li, W.M.H. Sachtler, E. Weitz, *Journal of Catalysis* 246 (2007) 413–427.
- [12] H. Dong, S. Shuai, R. Li, J. Wang, X. Shi, H. He, *Chemical Engineering Journal* 135 (2008) 195–201.
- [13] X. She, M. Flytzani-Stephanopoulos, *Catalysis Today* 127 (2007) 207–218.
- [14] H. He, X. Zhang, Q. Wu, C. Zhang, Y. Yu, *Catalysis Surveys from Asia* 12 (2008) 38–55.
- [15] S. Sumiya, M. Saito, H. He, Q. Feng, N. Takezawa, *Catalysis Letters* 50 (1998) 87–91.
- [16] A. Abe, N. Aoyama, S. Sumiya, N. Kakuta, K. Yoshida, *Catalysis Letters* 51 (1998) 5–9.
- [17] M. Boutros, J.M. Trichard, P. Da Costa, *Catalysis Letters* 52 (2009) 1781–1785.
- [18] T.A. Slatting, J.P. Kesan, *GCB Bioenergy* 4 (2012) 107–118.
- [19] J.H. Mack, S.M. Aceves, R.W. Dibble, *Energy* 34 (2009) 782–787.
- [20] J. Goldemberg, *Science* 315 (2007) 808–810.
- [21] C.R. Shen, E.I. Lan, Y. Dekishima, A. Baez, K.M. Cho, J.C. Liao, *Applied and Environmental Microbiology* 77 (2011) 2905–2915.
- [22] A. Cybulski, J.A. Moulijn, *Structure Catalysts and Reaction*, 2nd ed., Taylor & Francis Group, LLC, New York, 2006.
- [23] S.A. Solov'ev, P.I. Kirienko, *Catalysis in Industry* 2 (2010) 299–306.
- [24] J. Li, Sh. Kang, L. Fu, J. Hao, *Frontiers of Environmental Science & Engineering in China* 1 (2007) 143–146.
- [25] Patent US 2006/0228283 A1 (2006).
- [26] Patent US 7,541,010 B2 (2009).
- [27] E.V. Kul'ko, A.S. Ivanova, G.S. Litvak, G.N. Kryukova, S.V. Tsybulya, *Kinetics and Catalysis* 45 (2004) 714–721.
- [28] Y. Rozita, R. Brydson, A.J. Scott, *Journal of Physics: Conference Series* 241 (2010) 012096.
- [29] E.A. Paukshtis, *Infrared Spectroscopy in Heterogeneous Acid–Base Catalysis*, Novosibirsk, Nauka, 1992 (in Russian).
- [30] E.V. Kul'ko, A.S. Ivanova, A.A. Budneva, E.A. Paukshtis, *Kinetics and Catalysis* 46 (2005) 132–137.
- [31] G.A. Voronova, O.V. Vodyankina, V.N. Belousova, E.V. Bezrukov, L.N. Kurina, *Kinetics and Catalysis* 44 (2003) 652–656.
- [32] K. Shimizu, J. Shibita, H. Yoshida, A. Satsuma, T. Hattori, *Applied Catalysis B* 30 (2001) 151–162.
- [33] K.A. Bethke, H.H. Kung, *Journal of Catalysis* 172 (1997) 93–102.
- [34] N. Bogdanchikova, F.C. Meunier, M. Avalos-Borja, J.P. Breen, A. Pestryakov, *Applied Catalysis B* 36 (2002) 287–297.
- [35] B. Inceesungvorn, J. López-Castro, J.J. Calvino, *Applied Catalysis A* 391 (2011) 187–193.
- [36] F.C. Meunier, J.P. Breen, V. Zuzaniuk, M. Olsson, J.R.H. Ross, *Journal of Catalysis* 187 (1999) 493–505.
- [37] A. Iglesias-Juez, M. Fernandez-Garcia, A. Martinez-Arias, Z. Schay, Z. Koppány, A.B. Hungria, A. Fuerte, J.A. Anderson, J.C. Conesa, J. Soria, *Topics in Catalysis* 30/31 (2004) 65–70.
- [38] N.H. Kim, J.Y. Kim, K.J. Ihn, *Journal of Nanoscience and Nanotechnology* 7 (2007) 3805–3809.
- [39] D. Briggs, M.P. Seah, *Practical Surface Analysis – Auger and X-ray Photoelectron Spectroscopy*, vol. 1, 2nd ed., Wiley Interscience, 1990.
- [40] X. Zhang, H. He, H. Gao, Y. Yu, *Spectrochimica Acta, Part A* 71 (2008) 1446–1451.
- [41] S. Golay, R. Doepper, A. Renken, *Applied Catalysis A* 172 (1998) 97–106.
- [42] Y. Yu, H. He, Q. Feng, *Journal of Physical Chemistry B* 107 (2003) 13090–13092.
- [43] Q. Wu, Y. Yu, H. He, *Chinese Journal of Catalysis* 27 (2006) 993–998.
- [44] Q. Wu, H. He, Y. Yu, *Applied Catalysis B* 61 (2005) 107–113.
- [45] A. Sultana, M. Haneda, T. Fujitani, H. Hamada, *Catalysis Letters* 114 (2007) 96–102.

- [46] Y. Yan, Y. Yu, H. He, J. Zhao, *Journal of Catalysis* 293 (2012) 13–26.
- [47] Y.H. Yeom, M. Li, W.M.H. Sachtler, E. Weitz, *Journal of Catalysis* 238 (2006) 100–110.
- [48] Y. Yu, H. He, Q. Feng, H. Gao, X. Yang, *Applied Catalysis B* 49 (2004) 159–171.
- [49] H. Kannisto, K. Arve, T. Pingel, A. Hellman, H. Härelind, K. Eränen, E. Olsson, M. Skoglundh, D.Yu. Murzin, *Catalysis Science & Technology* 3 (2013) 644–653.
- [50] G.I. Golodets, *Heterogeneous Catalytic Reactions Involving Molecular Oxygen*, Elsevier, Amsterdam, 1983.
- [51] X. She, M. Flytzani-Stephanopoulos, *Journal of Catalysis* 237 (2006) 79–93.
- [52] J. Janas, W. Rojek, T. Shishido, S. Dzwigaj, *Applied Catalysis B* 123–124 (2012) 134–140.